Genetic deletion of the inflammation-regulated microRNA miR-146a increases exon-skipping mediated dystrophin restoration in Duchenne muscular dystrophy

Nikki M. McCormack[1], Kelsey A. Calabrese[1], Christopher B. Tully[1], Christopher R. Heier[1,2], Alyson A. Fiorillo[1,2]

[1]Center for Genetic Medicine Research, Children's National Hospital, Washington, District of Columbia, USA

[2]Department of Genomics and Precision Medicine, George Washington University School of Medicine and Health Sciences, Washington, District of Columbia, USA

***Correspondence:**

Alyson A. Fiorillo, PhD

Email: afiorillo@childrensnational.org

Tel: 202-545-2813

Keywords: Duchenne Muscular Dystrophy (DMD), Becker Muscular Dystrophy (BMD), dystrophin, exon skipping, microRNA, miR-146a-5p

Abstract

Duchenne muscular dystrophy (DMD) is a progressive muscle disease caused by loss of function mutations in the Dystrophin gene resulting in loss of dystrophin protein. Current DMD therapeutics use phosphorordiamidate morpholino oligomers (PMO) to skip over the frame-shifting exon during the splicing of the dystrophin pre-mRNA, resulting in translation of a truncated dystrophin protein product. While exon skipping therapies are promising, their potential has not been fully realized as increases in dystrophin protein have been minimal and highly variable in clinical trials. We previously described microRNAs that are upregulated in DMD and BMD muscle biopsies, bind to the dystrophin 3′UTR and inhibit dystrophin protein production. One of these dystrophin-targeting microRNAs, miR-146a, is regulated by the pro-inflammatory transcription factor NF-κB, is highly elevated in the muscles of dystrophin-deficient mice and is reduced by anti-inflammatory drugs. Here, we show that inflammation induces miR-146a expression in dystrophic myotubes. Using bioinformatics analysis, we validate previous findings that the dystrophin 3′UTR harbors a miR-146a binding site. An *in vitro* 3′UTR luciferase reporter assay further confirms that miR-146a inhibits dystrophin translation, while mutating the miR-146a binding site attenuates inhibition. In dystrophin-deficient mice we find that co-injection of an exon skipping PMO with miR-146a but not a control sequence reduces the extent of dystrophin positive fibers. To test the hypothesis that miR-146a is inhibitory to exon skipping dystrophin restoration, we generated a novel DMD double knockout mouse model with body-wide miR-146a deletion (*146aX* mice) and administered an exon 51 skipping PMO into the tibialis anterior (TA) muscles of *mdx52* and*146aX* mice. Excitingly, *146aX* TAs showed increased dystrophin protein versus *mdx52* as measured by capillary Western immunoassay and dystrophin-positive fiber quantification. Additionally, systemic PMO delivery increased dystrophin protein levels and increased the number of dystrophin-positive fibers in *146aX* versus *mdx52* muscles despite similar levels of skipped dystrophin transcripts in both groups. These data demonstrate genetic deletion of miR-146a is sufficient to increase dystrophin rescue via exon skipping. Our data suggests that antagomiR-mediated inhibition of miR-146a or other dystrophin targeting miRNAs could be a viable exon skipping DMD co-therapy and warrants further research.

Introduction

Duchenne muscular dystrophy (DMD) is a progressive muscle disease caused by out-of-frame mutations in the dystrophin (*DMD*) gene resulting in the complete loss of dystrophin protein (1). DMD is characterized by severe muscle weakness and chronic muscle inflammation leading to loss of ambulation and a shortened lifespan. Becker muscular dystrophy (BMD) is an allelic disease where the reading frame is preserved, resulting in production of a truncated dystrophin isoform that is expressed at lower and more variable levels (2-4). BMD is less severe and shows high variability both in clinical presentation and in levels of dystrophin protein even when comparing subjects harboring the same in-frame mutation (5-8). Interestingly, while dystrophin protein levels are variable and lower-than-normal in BMD, there are no differences in the amount of dystrophin mRNA detected in BMD as compared to unaffected/healthy muscles (7, 8).

Precision medicine strategies for DMD such as gene therapies and exon skipping antisense oligonucleotides (AOs) seek to convert a severe DMD genotype (dystrophin null) into a milder BMD (truncated dystrophin) phenotype. Specifically, exon skipping AOs act by binding to a complementary sequence on the dystrophin pre-mRNA to promote the exclusion of the frame-shifting exon. Currently four exon skipping phosphorodiamidate morpholino oligomers (PMOs) have received accelerated FDA approval; these target *DMD* exons 51 (Eteplirsen), 53 (Golodirsen, Viltepso) and 45 (Casimersen) (9-12). However, results from clinical trial data show low and variable dystrophin rescue. As an example, for the first approved exon skipping drug (Eteplirsen), the Western blot analysis shows an average of 0.93% dystrophin in treated muscles compared with a baseline value of 0.08% in biopsies of untreated Duchenne muscles (13). In the later Golodirsen clinical trial, mean dystrophin protein levels measured via Western blot are 1.019% of normal dystrophin levels despite 16.363% exon skipping (10, 14).

The disconnect between extent of DMD exon skipping (mRNA) and dystrophin protein levels point to post-transcriptional factors in the muscle that affect total dystrophin protein production via exon skipping. microRNAs (miRNAs) are elevated in a variety of muscle diseases; their canonical role is to fine-tune gene expression by binding to the 3′UTR of target genes and most often function to regulate protein levels post-transcriptionally via translation inhibition (7, 15-17). Previously, we identified several miRNAs (termed dystrophin targeting miRNAs or DTMs) that are elevated in DMD and BMD muscle biopsies and bind to the dystrophin 3'UTR *in vitro* (7). Several of these miRNAs, including the inflammation-associated miRNA miR-146a, are induced by tumor necrosis factor alpha (TNF-α) *in vitro*, suggesting regulation by NF-κB. Indeed, others have demonstrated NF-κB-specific regulation of miR-146a using cell culture studies (18) and bioinformatic analysis from ENCODE data (19). Importantly, our lab previously observed an inverse association between levels of exon-skipping mediated dystrophin restoration and miR-146a levels in the muscles of DMD model (*mdx)* mice (7). In a separate study, we describe a panel of 9 inflammatory miRNAs that are elevated in the *mdx* diaphragm and are reduced by vamorolone or prednisolone administration; included in this panel is the DTM miR-146a (20). Collectively, these data suggest that miR-146a is induced by inflammation, is elevated in dystrophic muscle and inhibits dystrophin protein production.

In the present study, we hypothesize genetic deletion of miR-146a will improve exon skipping-mediated dystrophin restoration in dystrophin deficient mice harboring a deletion of *Dmd* exon 52 (*mdx52*). Excitingly, following both intramuscular and systemic injection of PMO, we show deletion of miR-146a significantly increases dystrophin protein levels and the number of dystrophin-positive myofibers .

Methods

Mice

All animal studies were done in adherence to the NIH Guide for the Care and Use of Laboratory Animals. All experiments were conducted according to protocols within the guidelines and under approval of the Institutional Animal Care and Use Committee of Children's National Medical Center. *Mdx52* mice contain a deletion of exon 52 of the *Dmd* gene, resulting in the absence of full-length dystrophin. These mice on a C57/BL6 background are maintained in our own facility and were originally a kind gift from Dr. Shin'ichi Takeda. Male C57/BL6 mice were purchased from JAX laboratory (Bar Harbor, ME). *Bmx* mice contain an endogenous deletion of murine dystrophin exons 45-47, are maintained on a C57/BL6J background, and were previously characterized (8).

Muscle biopsies

Human biopsies used here were banked diagnostic biopsies obtained from the vastus lateralis muscle. Six BMD muscle biopsies were obtained from the Eurobiobank, Telethon Network Genetic Biobanks (GTB 12001D) (ID #: 2518, 3010, 3419, 4228, 7560, 7827). The remaining 4 BMD biopsies were obtained from our muscle biopsy bank as previously reported (ID#: 1141, 3212, 3255, 3461) (4, 7).

Generation of mdx/146a$^{-/-}$ mice

mdx52 on a C57/BL/6 background are bred in house (21). *miR-146a-/-* (B6.Cg-*Mir146*$^{tm1.1Bal}$/J) have been previously described (22) and were purchased from The Jackson Laboratory (Strain # 016239 and are on a C57/BL/6J background. To generate *mdx52* mice with deletion of miR-146a, mdx$^{-/-}$;146a$^{+/+}$ females were crossed with mdx$^{Y/+}$;146a$^{-/-}$ males to generate mdx$^{-/+}$:146a$^{+/-}$ females and mdx$^{Y/-}$;146a$^{+/-}$ males. mdx$^{-/+}$;146a$^{+/-}$ females and mdx$^{Y/-}$;146a$^{+/-}$ males were then

crossed to generate mdx$^{-/-}$;146a$^{-/-}$ breeders. Breeders were crossed to generate mdx$^{Y/-}$;146a$^{-/-}$ mice (*146aX*). For all experiments only males were utilized as DMD is an X-linked disorder. Genotyping for *mdx52* and miR-146a KO alleles was performed using TransnetYX with custom primers in Dmd exon 3 and a neomycin cassette for *mdx52* and with the standard JAX protocol for miR-146a-/- with forward primer 24664 (5′-GCT TAT GAA CTT GCC TAT CTT GTG-3′) and reverse primer 24665 (5′-CAG CAG TTC CAC GCT TCA-3′).

Cell Culture

Lipopolysaccharide (LPS) Treatment of mdx H2K Myotubes. H2K (H2Kb-tsA58) mdx myoblasts were cultured as previously described (23). For LPS-treatment, seeded myoblasts were differentiated into myotubes in 12-well plates (1.25 × 10^5 cells/well) with Matrigel at 37°C. After 4 days of differentiation, myotubes were then treated with LPS to induce inflammation (Thermo Fisher Scientific) at a dilution of 1:1,000. After 24 h, cells were lysed for RNA using TRIzol and expression of miR-146a and control RNAs was quantified by TaqMan Assay (Thermo Fisher Scientific).

Luciferase Reporter Assay. HEK293 cells were seeded in 24-well plates at a density of 4 × 10^4 or 8 × 10^4 cells/well and co-transfected 24 hours later with 200 ng dystrophin 3′ UTR or mutant reporter and with 50 nM miR-146a mimic (Life Technologies) with Lipofectamine 2000. Cells were harvested 24 hr. later according to Dual-Glow Luciferase Reporter Assay System protocol (Promega) where renilla luciferase was the main readout (3′UTR) and firefly luciferase served as the internal control.

miR-146a mimic injections

mdx52 mice were anesthetized with isoflurane and 2 µg of PMO was injected into each tibialis anterior. Mice were co-injected with either 10 µg of a miR-146a mimic or control sequence

(ThermoFisher scientific). Mice were euthanized two weeks after intramuscular injection and muscles were harvested and frozen.

PMO Treatment

The *Dmd* exon 51 skipping PMO utilized here is the sequence for Eteplirsen modified for the mouse genome and has been previously reported (24). The sequence is: (5′-CTCCAACAGCAAAGAAGATGGCATTTCTAG-3′) and was synthesized by Gene Tools.

Intramuscular Injections. For intramuscular injections, 12- week- old mice were anesthetized with isoflurane and 2 µg of PMO was administered into each tibialis anterior. Mice were euthanized two weeks after intramuscular injection and muscles were harvested and frozen.

Intravenous Injections. For intravenous injections, 15-week-old mice were anesthetized with isoflurane and 400 mg/kg PMO was administered via retroorbital injection. A second IV dose of PMO (400 mg/kg) was given seven days later. Mice were euthanized two weeks after the second injection and muscles were harvested and frozen.

Capillary Gel Electrophoresis (Wes)

Muscles were dissected and frozen in liquid-nitrogen cooled isopentane. 8 µm sections were lysed in High SDS buffer containing 0.02% EDTA (pH 8.0), 0.075% Tris-HCL (pH 6.8), and protease inhibitors. Capillary Western immunoassay (Wes) analysis was performed according to manufacturer's instructions using 66–440 kDa Separation Modules (ProteinSimple). In each capillary 0.2mg/mL protein was loaded for analysis with antibodies to dystrophin (Abcam #ab15277, dilution 1:15) or vinculin (Abcam #ab130007, dilution 1:100), and anti-rabbit secondary (ProteinSimple #042-206). Compass for SW software was used to quantify chemiluminescence data.

qRT-PCR

Dmd exon skipping. Total RNA was extracted from muscle samples by standard TRIzol (Life Technologies) isolation. Purified RNA (400ng) was reverse-transcribed using Random Hexamers and High-Capacity cDNA Reverse Transcription Kit (Thermo Fisher). Skipped and non-skipped *Dmd* transcripts were measured by qRT-PCR using TaqMan assays and Taqman Fast Advanced MasterMix (Thermo Fisher) on an ABI QuantStudio 7 Real-Time PCR machine (Applied Biosystems). A custom TaqMan probe for the skipped *Dmd* product (Thermo Fisher) was designed to amplify the splice junction spanning *Dmd* exons 50-53. TaqMan probe Mm01216492_m1 (Thermo Fisher) that amplifies the region spanning *Dmd* exons 2–3 was utilized to calculate non-skipped *Dmd* transcript levels. Percent exon skipping was calculated based on the corresponding ΔCt values for skipped and total *Dmd* transcript normalized to *Hprt* (Mm01545399_m1; Thermo Fisher) and *18S* (Mm03928990_g1; Thermo Fisher) mRNA, using the following equation: [(Average of triplicate reactions of skipped *Dmd*)/(Average of triplicate reactions of skipped *Dmd*+Average of triplicate reactions of non-skipped *Dmd*)] * 100.

miRNAs. Total RNA was converted to cDNA using multiplexed RT primers and High Capacity cDNA Reverse Transcription Kit (ThermoFisher; Carlsbad, CA). miRNAs were then quantified using individual TaqMan assays on an ABI QuantStudio 7 real time PCR machine (Applied Biosystems). Assay IDs include: miR-146a 000468 and controls sno202 001232, RNU48 001006. miR-146a levels were normalized to the geometric mean of controls.

Immunofluorescence

Muscles were mounted on cork, flash frozen, and sectioned (8 μm) onto slides. For most immunofluorescence experiments muscle sections were fixed in ice cold acetone for 10 minutes. Slides were washed with 1X PBST (0.1% Tween 20), blocked for 1 hour (1X PBST with 0.1% Triton X-100, 1% BSA, 10% goat serum, and 10% horse serum), washed 3 times,

then exposed to primary antibodies overnight at 4ºC: anti-dystrophin 1:150 (Abcam, #ab154168) and anti-laminin-2 1:100 (Sigma-Aldrich, Cat. #L0663). Secondary antibodies included: goat anti-rabbit 568 1:400 (ThermoFisher, #A-11036) and donkey anti-rat 488 1:400 (ThermoFisher, #A-21208). Wheat germ agglutinin (WGA) conjugated to Alexa Fluor 647 (Life Technologies, MA) was prepared as 1 mg/ml stock solutions and used at a 1:500 dilution in PBS. Coverslips were mounted using Prolong Gold Mounting Medium with DAPI. Slides were imaged using an Olympus VS-120 scanning microscope at 20X.

Image Analysis

Images in each experiment were thresholded to the same levels, and then exported as PNG files and blinded using randomly assigned number IDs. To determine % dystrophin-positive fibers, the total number of myofibers (marked by either wheat-germ agglutinin or laminin staining) were counted manually using ImageJ. Dystrophin positive fibers were additionally counted, and the percentage of dystrophin-positive fibers were determined by the following formula: dystrophin-positive fibers/ total fibers x 100. For secondary analysis dystrophin high and low fiber percentages were determined based on a visual standard (Fig S2C).

Results

Inflammation-regulated miR-146a is elevated in dystrophic muscle

We previously reported that DTMs, including miR-146a, inhibit dystrophin protein production *in vitro* and are inversely related to exon skipping-mediated dystrophin restoration *in vivo* (7). One particular miRNA, miR-146a, was found to be highly elevated in BMD, DMD and *mdx* muscle (7) and analysis of ENCODE data shows it is regulated by the pro-inflammatory transcription factor NF-κB (19).

The miR-146a locus is found on chromosome 5q33.3 and is located in a cluster along with the long non-coding RNA MIR3142HG. miR-146a is evolutionarily conserved across species, as demonstrated by alignment of the miR-146a sequence from human, chimpanzee, baboon, dog, mouse, xenopus and zebrafish **(Figure 1A**). Evaluating levels of miR-146a from Becker muscular dystrophy human biopsies with deletion of *DMD* exons 45-47, we previously found miR-146a levels are higher in biopsies from patients with low dystrophin levels (<20%) (**Figure 1B**, data from (7).) Plotting miR-146a levels versus dystrophin protein levels in these same BMD 45-47 biopsies, we observed a significant inverse correlation between miR-146a levels and the percent of dystrophin protein in BMD biopsies ($r=-0.6365$, $p<0.01$, **Figure 1B′).** Elevated miR-146a levels in dystrophic muscle are corroborated by our analysis of previously published data from Eisenberg et. al (15) that shows elevated miR-146a in DMD, and BMD patient biopsies (**Figure 1C**). We analyzed the diaphragm, tibialis anterior, quadriceps, gastrocnemius and triceps muscles from 3-month-old *mdx52* mice and found elevated levels of miR-146a in all muscles analyzed (**Figure 1D**). We also analyzed miR-146a in the *bmx* mouse model of BMD with deletion of murine *Dmd* exon 45-47 (8) at 5 months of age, and saw significantly elevated levels in the quadriceps, gastrocnemius and triceps **(Figure 1E**).

Previous studies have demonstrated that miR-146a is regulated by NF-κB in THP-1 macrophage cells (18); corroborating this, we show high induction of miR-146a in *mdx*

myotubes (*mdx H-2K*) upon lipopolysaccharide (LPS)-induced inflammation (**Figure 1F**). Overall, these findings suggest miR-146a is upregulated in the muscle of BMD and DMD patients, as well as in mouse models of these diseases, and is induced by inflammatory stimuli in dystrophic myotubes *in vitro*.

miR-146a inhibits dystrophin translation

To validate our previous finding that miR-146a regulates dystrophin translation, we utilized the scanMiR toolkit (25) to identify putative miR-146a binding sites or microRNA response elements (MREs) within the human dystrophin 3′UTR (**Figure 2A, B**). scanMiR identified multiple types of binding sites relative to the miR-146a seed sequence which is located at nucleotides 2-7 of the miRNA sequence (26). These site types included a 7mer-m8 (perfect complementarity of the seed sequence to the UTR and complementarity extending to nucleotide 8), a 6mer-A1, (seed sequence complementarity at positions 3-7 and additional complementarity at nucleotide 8), a 6mer-A1 (seed sequences at positions 2-6 and an A at position 1), a wobbled 8mer (A at position 1, seed sequence complementarity interrupted by a single mismatch and additional complementarity at position 8), and several non-canonical binding sites (26). In total, scanMiR predicted 17 binding sites, although only two showed strong dissociation constants (-log K_d <-3). The miR-146a MRE with the strongest predicted dissociation constant (log K_d -4.425) is located at position 1281-1288 of the 3′UTR (**Figure 2B, 2C**).

Using this information, we next utilized a dystrophin 3′UTR luciferase reporter (WT) or a reporter where the 3'UTR MRE was mutated (Mut) to eliminate base-pairing of miR-146a at position 2,3 and 6-8 (**Figure 2C**). WT and Mut constructs were transfected into HEK293T cells with either a control or miR-146a mimic sequence. Analogous to our previously reported results (7), miR-146a significantly reduced WT 3′UTR luciferase expression while mutation of the miR-146a MRE attenuated this inhibition (**Figure 2D**). To support this *in vitro* data, we utilized the

mdx52 mouse, which is amenable to exon 51 skipping. We performed intramuscular TA injections with 2 mg of an exon 51 skipping PMO and 10 mg of either a miR-146a mimic or a control sequence (n=10 per group). Fourteen days post-injection muscles were harvested, and dystrophin immunofluorescence was performed. Using qRT-PCR, we observed significantly increased miR-146a in muscles co-injected with the miR-146a mimic sequence (**Figure S1**). Additionally, we found a significant decrease in dystrophin positive fibers in muscles co-injected with miR-146a as compared to muscle injected with a control sequence (36.1% decrease, $p<0.05$, **Figure 2E, E′, Fig S1**). Together these data suggest that miR-146a binds to the dystrophin 3′UTR to regulate its translation and high levels of miR-146a are inhibitory to successful dystrophin rescue via exon skipping.

Body-wide deletion of miR-146a increases dystrophin rescue in mdx52

To investigate the potential therapeutic implications of miR-146a, we generated *mdx52* mice with body-wide deletion of miR-146a by crossing several generations of *mdx52* and miR-*146a-/-* mice both *on* a C57/BL/6 background (*146aX*). **(Figure 3A**). Deletion of miR-146a was determined by genotyping and validated by qRT-PCR of the gastrocnemius muscle (**Figure 3B**).

We next injected an exon 51 skipping PMO (2µg) into the TAs of *mdx52* and *146aX* mice. Fourteen days post-injection muscles were harvested and analyzed for extent of exon skipping and dystrophin protein (**Figure 3C**). To analyze exon skipping we performed qRT-PCR on both *Dmd* exon 2 (total *Dmd* transcript levels) and the novel junction between *Dmd* exon 50 and 53 (skipped *Dmd* transcript levels) to determine the percent exon skipping achieved in each muscle as we previously described (27). Levels of exon skipping ranged between 0.5% and 7%, and there were no significant differences observed between RNA from *mdx52* and *146aX* TAs ($p=0.48$, **Figure 3D**). We next performed capillary Western immunoassays (Wes), as dystrophin quantification using this method has proven to be highly sensitive, reproducible, and quantitative over a large dynamic range [28]. While no transcript levels differences were observed in exon

skipping, Wes protein quantification revealed a significant increase in dystrophin levels in *146aX* muscles (~19% increase, p<0.05, **Figure 3E, E′**). Supporting this, dystrophin immunofluorescence showed a greater than 2-fold increase in dystrophin positive fibers in *146aX* TAs (p<0.01, **Figure 3F, F′**).

We next performed retroorbital injections of a high dose PMO into 15-week-old *mdx52* or *146aX* mice (400 mg/kg) n=4 mice per group. One week later we performed a second high dose injection (400 mg/kg). Mice were sacrificed 2 weeks after the final dose and diaphragm (Dia), tibialis anterior (TA), quadriceps (Quad,) gastrocnemius (Gastroc), Triceps (Tri) were collected for RNA and protein analysis (**Figure 4A**). Similar to intramuscular injections, when we analyzed the extent of exon skipping across muscles via qRT-PCR, no significant differences were observed between groups (**Figure 4B**), however, there was a non-significant trend towards increased exon skipping in the *mdx52* versus *146aX* muscles. Conversely, analysis of dystrophin protein levels via Wes showed significantly increased dystrophin in *146aX* muscles as compared to *mdx52* (~55% increase, p<0.05, **Figure 4C, C′ Figure S2A**). To account for differences in PMO delivery between muscles and genotypes, we also normalized dystrophin protein levels as measured by Wes, to exon skipping RNA levels measured by qRT-PCR. Interestingly, using this method to normalize dystrophin protein we found that on average, 146aX muscles have a 2.4-fold increase in dystrophin protein per “skipped” transcript (**Figure 4D**). Quantification of dystrophin positive fibers showed higher dystrophin restoration in *146aX* muscles (43.5% increase p<0.05, **Figure 4E, E′ Figure S1B**); which persisted even after normalizing to percent exon skipping, here showing a 3.5-fold increase in dystrophin positive fibers per “skipped” transcript (**Figure 4F**). Additionally, we partitioned dystrophin positive fibers as either “high” or “low” and performed reanalysis of fiber quantification data (**Figure S2C**) Interestingly, we found that while the extent of bright fibers was not significant between groups (p=0.06), faint fibers were significantly more abundant in *146aX* muscles (**Figure S2D**),

suggesting that lack of miR-146a stabilized skipped dystrophin transcripts and more protein is continuing to be produced from those transcripts. Collectively, this data supports the idea that reducing miR-146a can markedly improve exon-skipping-mediated dystrophin restoration.

Discussion

In the study presented here, we find miR-146a inhibits dystrophin protein levels *in vitro* and *in vivo* and is induced by inflammation in muscle. Excitingly, we also find that delivery of an exon 51 skipping PMO in *mdx52* mice with genetic deletion of miR-146a increases local dystrophin protein levels after intramuscular injection and increases body wide dystrophin protein levels after systemic injection. To our knowledge, this is the first report showing that genetic deletion of a single miRNA can increase dystrophin protein in combination with administration of an exon skipping PMO.

This work is relevant and timely given current clinical trial data for exon skipping PMOs. By using a genetic deletion model to ablate miR-146a in *mdx52* mice, this pilot study provides proof-of-principal that targeting miR-146a could potentially lead to increased dystrophin rescue in DMD exon skipping. Specifically, we show that the extent of dystrophin positive fibers increases from ~15 to 25%, and that on average, loss of miR-146a enables ~2.5 to 3.5-fold more dystrophin protein to be expressed from each “skipped transcript.” This suggests that miR-146a deficiency results in more efficient dystrophin protein production. We observed more myofibers expressing a “low” level of dystrophin via immunofluorescence. This could potentially be explained by the fact that mice were sacrificed 2 weeks after the final PMO injection and that fibers with “low” dystrophin were just starting to accumulate sufficient dystrophin protein from skipped transcripts to be detected in immunofluorescence. Potentially, if mice have been sacrificed 4-6 weeks after the final PMO injection, it would have allowed more time for dystrophin protein to accumulate from “skipped” transcripts which would have yielded a greater difference between *mdx52* and *146aX* genotypes. Future studies will determine how miR-146a deficiency affects the extent of *mdx* muscle turnover, the persistence of skipped transcripts and the overall accumulation of dystrophin protein after PMO administration.

Our data show that deletion of miR-146a results in significant increases in dystrophin protein as measured via Wes and immunofluorescence. The extent of dystrophin rescue reported from DMD exon skipping clinical trials for Eteplirsen, golodirsen and casimersen is, on average, about 0.9-1.9% of unaffected levels ((10, 13), NCT02500381*)*. The target amount of dystrophin restoration needed to show a functional benefit in DMD is still unclear. Some reports using severe mouse models show 4% dystrophin is sufficient for improved muscle function and survival (28-30). Other reports show that 20% dystrophin improves symptoms (31) and 15% could be sufficient to protect against contraction-induced injury in DMD model mice but more than 40% dystrophin is needed to also improve muscle force (32). Additionally, we recently found that BMD model mice expressing 30-50% dystrophin (in-frame deletion of *Dmd* exons 45-47) exhibit susceptibility to contraction-induced injury and harbored motor function deficits (8). Based on these collective data, it is unlikely that the extent of dystrophin rescue observed in the Eteplirsen, golodirsen and casimersen clinical trials is sufficient to provide a clinical meaningful benefit. The most recent clinical data for the NS Pharma drug Viltolarsen shows more promising preliminary data, with 5.9% dystrophin measured in muscle biopsies (33). Even with the increased efficacy of viltolarsen, improvement in the extent of dystrophin restoration is necessary to yield the full potential of exon skipping therapeutics in DMD. Our study here suggests that targeting miR-146a could potentially contribute to that overall goal.

Cacchiarelli et. al.(16) was the first to show that a microRNA that is significantly upregulated in *mdx* muscles, miR-31, could target the dystrophin 3′UTR and inhibit dystrophin protein production. Our lab later built on this data using BMD del45-47 biopsies and described seven additional miRNAs that target dystrophin, including miR-146a. Following the initial miR-31 publication, Wells and Hildyard performed intraperitoneal injections of an exon 23 skipping vivo-PMO alone or in combination with a miR-31 protector sequence (to prevent miR-31 binding to the dystrophin 3'UTR) or a "scrambled protector" sequence (34). While they observed increased

dystrophin in cell culture experiments by inhibiting or blocking miR-31, this result did not translate *in vivo* (34). There were, however, limitations to this study as the authors discuss. Specifically, they postulated that delivery of the vivo-morpholinos overall was low, with almost no delivery to hindlimbs, and modest delivery to the diaphragm and less to the abdominal wall, and therefore it wasn't clear whether the miR-31 target blocking strategy failed or the co-delivery of both the exon skipping PMO and the target blocker was too low to observe any measurable differences in dystrophin protein. Based on their report and interpretation, here, we chose to use a genetic approach to ablate expression of miR-146a so that the efficiency of delivery of an inhibitor or blocking sequence was not a confounding factor in analysis. Moving forward we will utilize an enhancer strategy to determine how co-delivery of a miR-146a inhibitor or target blocking sequence with an exon skipping PMO affects dystrophin protein restoration in dystrophic mice.

The aim of this pilot study was to determine if loss of miR-146a could improve exon skipping-driven dystrophin protein restoration as the primary outcome. Therefore, in this initial study we did not perform functional analysis, or additional secondary outcome measures, and utilized a high dose PMO injection. While it is well established that weekly PMO injections increase exon skipping, we felt that a slight modification of our previous work (single 800 mg/kg injection) (35) would be better suited to examine the effects of miR-146a on dystrophin protein restoration. Since using a high dose PMO is costly, large sample sizes were cost-prohibitive for these studies. To increase power, we therefore pooled muscle groups. Besides increasing power of the study, this analysis makes sense for two reasons. First, we have previously found that giving a single high dose PMO yields high intra-variability in different muscles of a single mouse (35). Second, as the goal of DMD exon skipping is to increase body wide dystrophin rescue, merely choosing one muscle for analysis does not provide the entire picture of successful dystrophin rescue. Because of the success of this initial study, in future work, we will

perform long term low dose PMO administration in a greater number of mice to mirror what has been done in the clinic to date.

Elevated levels of miR-146a have been described in numerous other chronic inflammatory and muscle disorders including myositis (36), Miyoshi myopathy (15), limb girdle muscular dystrophy (15), FSHD (37), rheumatoid arthritis (38), Sjogren's syndrome (39), inflammatory bowel disease (19, 40, 41), and asthma (42) suggesting it plays a role in diseases where inflammation persists. Previous studies have reported that miR-146a is rapidly elevated in response to inflammatory stimuli, but then "turns off" the NF-κB signaling pathway via binding to the *Traf6* and *Irak1* 3′UTRs (18, 43, 44). Because of this, it is generally regarded as "anti-inflammatory." However, more recent work has described a mechanism where exogenous miR-146a-5p, but not its duplex precursor, is "pro-inflammatory" and induces inflammation via activation of TLR7 while it's duplex precursor functions as part of a negative feedback loop to "turn off" NF-κB (45). This work shows that the narrow definition of a miRNA such as miR-146a as either anti- or pro-inflammatory is perhaps too reductive and more work is required to fully delineate the comprehensive role of each microRNA in both a healthy and a disease state.

It should be noted that another group also generated *mdx:miR-146a-/-* mice (46), however, the overall aim of that work was significantly different from the work we present here. The previous study sought to test the hypothesis that miR-146a is anti-inflammatory and that genetic deletion of miR-146a in *mdx* would worsen disease; after analysis they reported no signficant differences between the *mdx* mice with or without miR-146a expression. The data we present here demonstrates that miR-146a deletion benefits dystrophin rescue in *mdx52* mice treated with an exon 51 skipping PMO. While we have not yet characterized the functional or molecular differences between *mdx52* and *146aX* mice we wanted to comment on a major limitation in the experimental design from the previous aforementioned work. Specifically, Bronisz-Budzynska et. al. (46) crossed *mdx23* mice (C57BL/10ScSnJ background) to *miR-146a-*

/- mice (C57BL/6J background) to generate *mdx:146a-/-* mice on a mixed BL/10:BL/6 background; the use of different genetic backgrounds thus reduces confidence in their conclusions for *mdx23* and *mdx:miR-146a-/-* comparisons. For our studies we crossed *mdx52* mice and *miR-146a-/-* both on a C57BL/6 genetic background, thus the resulting *146aX* mice are also on a C57BL/6 background. Our lab is currently characterizing the muscles and function of WT, *miR-146a-/-*, *mdx52* and *146aX* mice on a C57BL/6 background; we hope these ongoing studies will yield more insight into the role of miR-146a in states of either acute or chronic inflammation.

Interestingly, we found elevated miR-146a in murine myositis muscle and human muscle biopsies of inclusion body myositis (36). In these same muscles, we observed reduced dystrophin staining via Western blot as well as reduced and discontinuous dystrophin staining (36). Thus, it is possible that DTMs such as miR-146a contribute to a secondary dystrophin deficiency that would impair overall muscle function and the therapeutic targeting of this inflammation-regulated miRNA could be beneficial in the context of other muscle disorders.

One potential way to improve DMD exon skipping outcomes is to harness miRNA therapeutics as a combination therapy with the goal of inhibiting miR-146a-5p levels to enable increased dystrophin protein production from skipped dystrophin transcripts. This strategy could also potentially be applied as a stand-alone therapy in BMD where lower-than-normal levels of dystrophin are observed in muscle. There are a few different ways in which miR-146a inhibition or reduction can be achieved. These include the use of 1) a miR-146a inhibitor (anti-miR), 2) an oligonucleotide that prevents miR-146a from binding to the dystrophin 3′UTR (target blockers or blockmiRs), or 3) a small molecule inhibitor. Currently, there are several anti-miR therapeutics in clinical trials that show promising preliminary results (reviewed in (47)) including CDR132L, a locked nucleic acid (LNA) targeting miR-132 in heart failure (48), Miravirsen/SPC3649, an LNA targeting miR-122 in patients with chronic hepatitis C virus (49), and MRG-110, an LNA targeting miR-92a to benefit wound failure (50). Additionally, in myotonic dystrophy (DM1)

preclinical studies, using either a miR-23b antagomiR(51) or a peptide-conjugated blockmiR to prevent miR-23 binding to MBNL (52), have resulted in improved muscle function in mouse models. We have also observed reduced levels of miR-146a through treatment with anti-inflammatory small molecules, either vamorolone or prednisone, in *mdx* mice (7, 20). While current inclusion criteria for DMD exon skipping therapeutics includes corticosteroid use, investigating the optional dose and drug treatment that yields optimal DTM reduction and corresponding dystrophin protein increases could help inform DMD treatment.

In conclusion, the data presented here shows that miR-146a deletion increases levels of therapeutic dystrophin protein restoration without affecting the extent of skipped dystrophin transcript levels. The increase in dystrophin protein but not dystrophin transcript levels makes sense given our previous data in BMD biopsies and in BMD model mice showing that, while dystrophin transcript levels are the same, dystrophin protein levels are significantly reduced and negatively correlate with levels of miR-146a and other DTMs (7, 8), and that most often miRNAs inhibit translation but do not promote mRNA decay (17). These data provide a strong rationale for investigating how the therapeutic targeting of miR-146a and other DTMs may impact dystrophin protein levels in DMD exon skipping.

Figures and Figure Legends

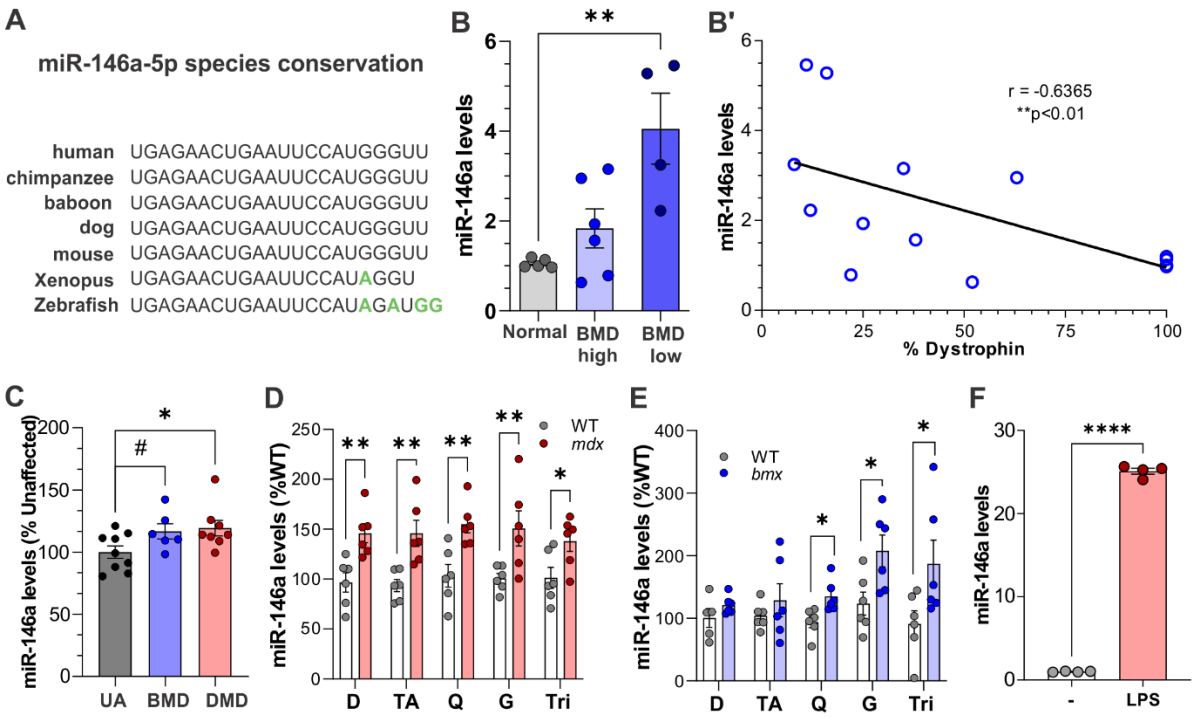

Figure 1. miR-146a is significantly elevated in BMD and DMD patients and model mice.

(**A**) The sequence of miR-146a-5p is conserved across species. Note that in mammals there is 100% conservation. (**B**) miR-146a levels are elevated in BMD patients with low dystrophin (<20% dystrophin of unaffected individuals). n=5 normal, 6 “BMD high” and 4 “BMD low”; ANOVA, **p<0.001, adapted from (7). (**B'**) Dystrophin protein and miR-146a levels are inversely correlated in BMD patients. Spearman correlation, r=-0.6365, **p<0.01. Adapted from (7). (**C**) miR-146a levels are significantly elevated in both BMD and DMD patients (taken from raw data presented in (15)). ANOVA, #p<0.1, *p<0.05. (**D**) miR-146a levels are significantly increased in *mdx52* mouse diaphragm (D), tibialis anterior (TA), quadriceps (Q), gastrocnemius (G), and triceps (Tri). n=6/group; Two-way ANOVA, **p<0.01, *p<0.05. (**E**) miR-146a levels in *bmx* mouse diaphragm (D), tibialis anterior (TA), quadriceps (Q), gastrocnemius (G), and triceps (Tri) and significantly increased in the latter 3 muscles. n=6/group, Two-way ANOVA, *p<0.05. (**F**)

miR-146a is significantly elevated in mdx H2K myotubes treated with LPS (n=4/group) Student's t-test, ****p<0.0001. Data represented as mean ± S.E.M.

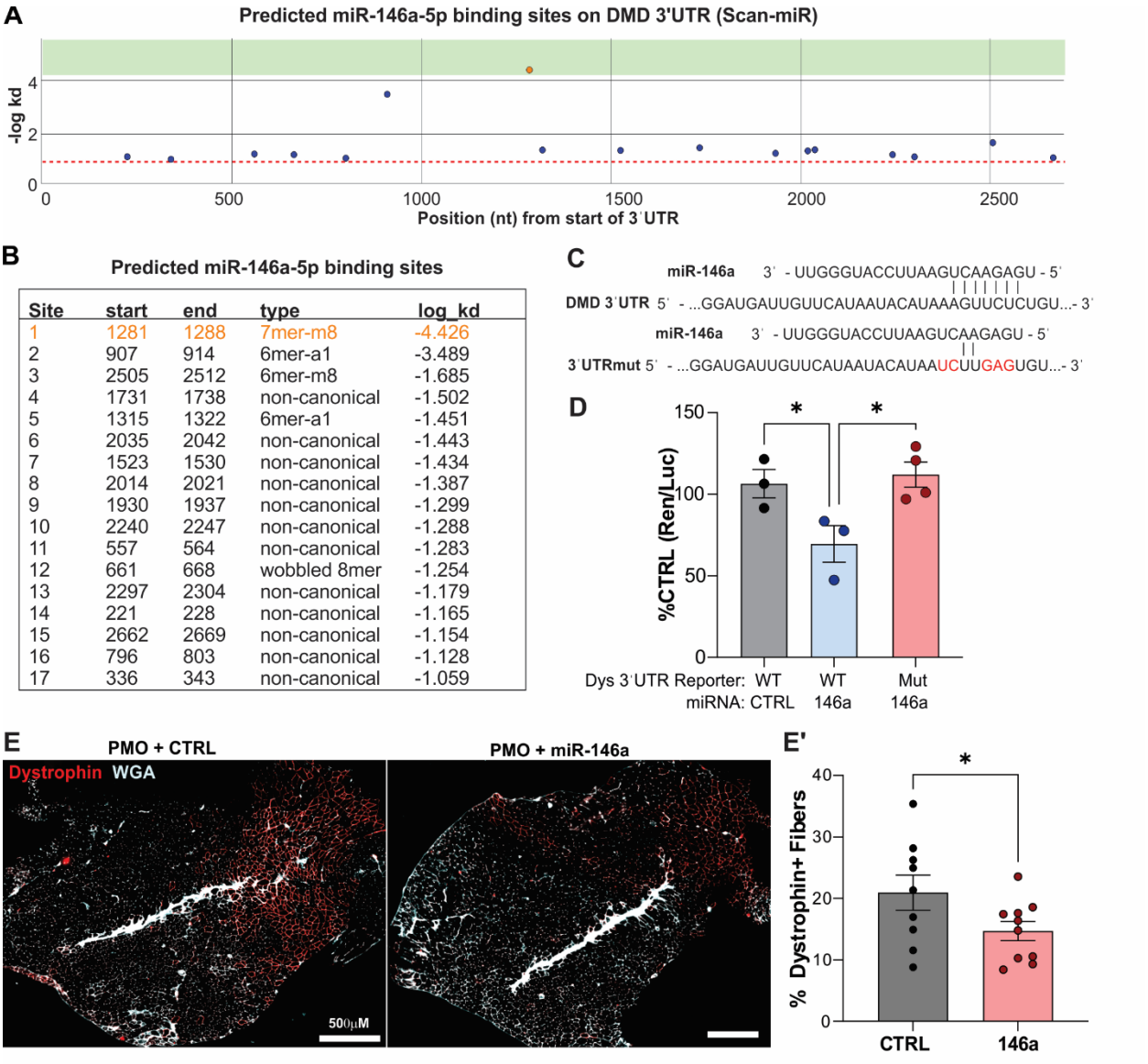

Site	start	end	type	log_kd
1	1281	1288	7mer-m8	-4.426
2	907	914	6mer-a1	-3.489
3	2505	2512	6mer-m8	-1.685
4	1731	1738	non-canonical	-1.502
5	1315	1322	6mer-a1	-1.451
6	2035	2042	non-canonical	-1.443
7	1523	1530	non-canonical	-1.434
8	2014	2021	non-canonical	-1.387
9	1930	1937	non-canonical	-1.299
10	2240	2247	non-canonical	-1.288
11	557	564	non-canonical	-1.283
12	661	668	wobbled 8mer	-1.254
13	2297	2304	non-canonical	-1.179
14	221	228	non-canonical	-1.165
15	2662	2669	non-canonical	-1.154
16	796	803	non-canonical	-1.128
17	336	343	non-canonical	-1.059

Figure 2. miR-146a targets the dystrophin 3′UTR and reduces exon skipping-mediated dystrophin restoration. (**A-B**) Predicted miR-146a-5p binding sites in the human *DMD* 3'UTR. (**A**) Scan-miR was used to search for putative miR-146a-5p binding sites within the human dystrophin 3′UTR sequence. The y axis denotes the dissociation constant (-log Kd), and the x axis denotes the location on the dystrophin 3′UTR in the 5′ to 3′ direction. (**B**) List of 17 putative miR-146a binding sites in the *DMD* 3' UTR; orange denotes the strongest binding site and the one that was mutated in the luciferase construct in (**C**). The predicted binding sites include: a 7mer-m8 where there is perfect complementarity of the seed sequence with the UTR and this

complementarity extends to nucleotide 8; a 6mer-A1 where there is seed sequence complementarity at nucleotide positions 3-7 and additional complementarity at nucleotide 8; a 6mer-A1, where the seed sequence shows complementarity to the UTR at positions 2-6 and additionally possesses an adenosine (A) at position 1; an wobbled 8mer, where there is an adenosine position 1, seed sequence complementarity at position 2-7 that is interrupted by a single mismatch and additional complementarity at position 8 and several non-canonical binding sites (26). (**C**) Schematic showing the binding site of miR-146a on the *DMD* 3' UTR (top) and the base pairing of miR-146a with the *DMD* 3' UTR when the binding site is mutated (bottom). (**D**) A luciferase reporter assay was used to examine miR-146a binding to the WT and mutant *DMD* 3' UTR in HEK-293T cells. Transfection with miR-146a significantly reduces reporter activity in cells with WT *DMD* 3' UTR whereas there is no reduction in reporter activity in cells with the mutated *DMD* 3' UTR. n=3-4, ANOVA, *p<0.05. (**E**) The TAs of *mdx52* mice were injected with 2μg of exon skipping PMO and 10μg of either control or miR-146a. TA cross sections were stained for dystrophin (red) and wheat germ agglutinin (white). (**E'**) Quantification of dystrophin positive fibers; significantly fewer dystrophin-positive myofibers were observed in muscles co-injected with miR-146a compared to control. n=9-10, Student's t-test, *p<0.05. Data represented as mean ± S.E.M.

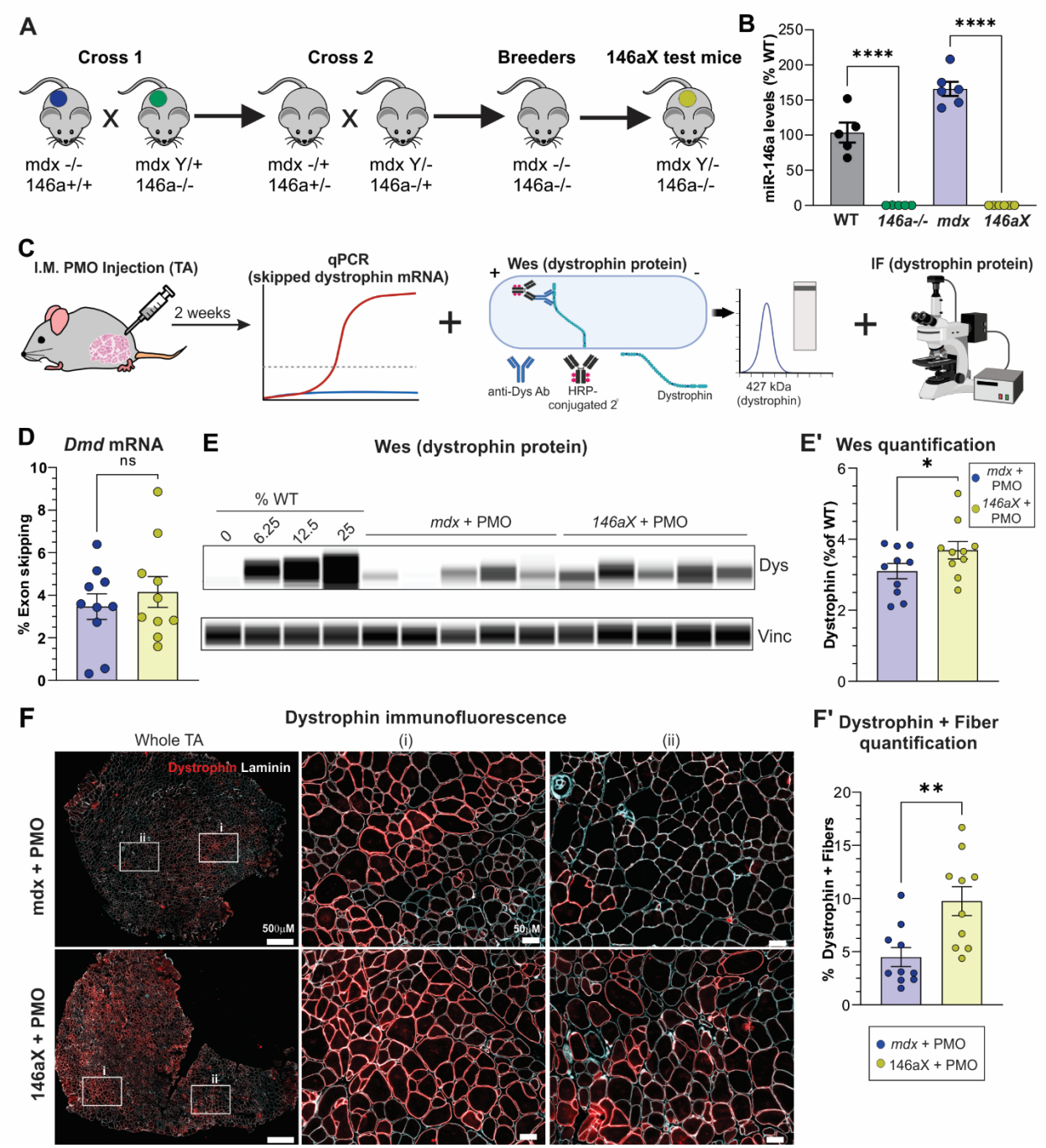

Figure 3. Deletion of miR-146a significantly increases dystrophin restoration in *mdx52* mice treated with intramuscular PMO. (**A**) Breeding schematic to develop *mdx52*:*146a-/-* (*146aX*) mice. (**B**) miR-146a levels in the gastrocnemius muscles of WT, 146a-/-, *mdx*, and *146aX* mice. *146a-/-* and *146aX* mice have no detectable levels of miR-146a via qRT-PCR. n=6/group, ANOVA, ****p<0.0001. (**C**) Schematic of intramuscular PMO injection experimental

design. *mdx* and *146aX* tibialis anterior muscles (TAs) were injected with 2ug of an exon 51 skipping PMO. 2 weeks post-injection muscles were harvested for analysis. n=10 muscles/group and 5 mice per group. Wes = Western capillary immunoassay, IF = immunofluorescence. (**D**) qRT-PCR was performed quantify % exon skipping in PMO-injected *mdx52* and *146aX* TAs as previously described (27). Exon skipping efficiency is not significantly between *mdx52* and *146aX* TAs. (**E**) Capillary-based immunoassay (Wes) was used to quantify levels of dystrophin protein. (**E'**) Dystrophin is significantly increased in *146aX* mice injected with PMO compared to *mdx* mice. (**F**) Immunofluorescence showing dystrophin staining in the TA of mdx and *146aX* mice with intramuscular PMO. (i) shows a zoomed in area of high dystrophin rescue and (ii) shows a zoomed in area of low dystrophin rescue. Bars = 500μm and 50 μm respectively. (**F'**) Quantification of dystrophin-positive myofibers. The percentage of dystrophin-positive myofibers following PMO injection is significantly increased in *146aX* mice compared to mdx mice. Images were blinded during quantification. Data represented as mean ± S.E.M. ns $p>0.05$, *$p\leq0.05$, **$p\leq0.01$, ****$p\leq0.0001$.

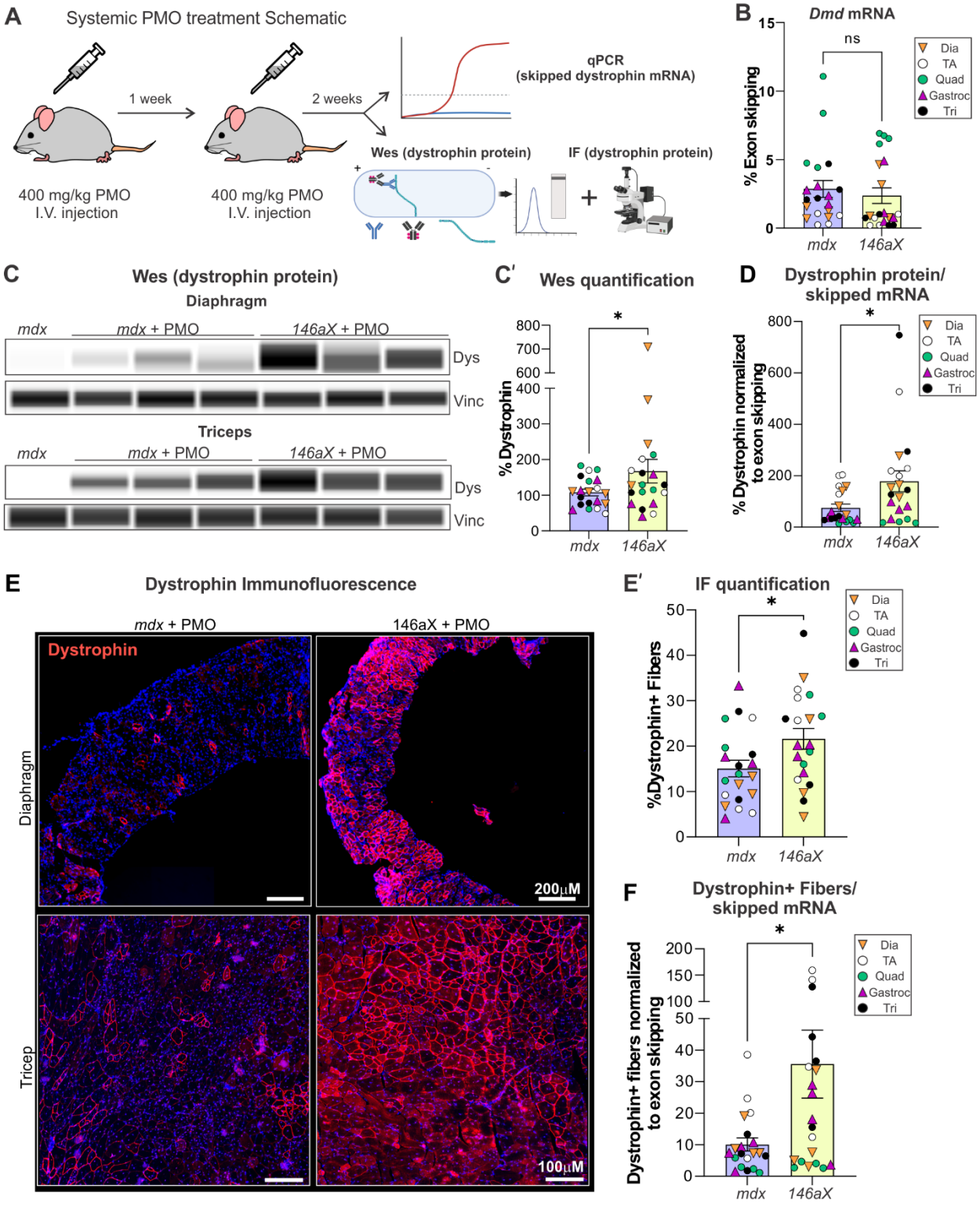

Figure 4. Deletion of miR-146a significantly increases dystrophin restoration in *mdx52* mice treated with systemic PMO. (**A**) Schematic of experimental design for systemic PMO

injections in *mdx* and *146aX* mice. Mice were administered systemic PMO via the retroorbital sinus (400 mg/kg, exon 51 skipping PMO) at 12 weeks of age. One week later a second 400mg/kg PMO injection was performed. Mice were sacrificed 2 weeks after second injection and muscles were harvested for analysis of skipped *Dmd* mRNA and dystrophin protein levels using a Western capillary immunoassay (Wes) and immunofluorescence (IF). n=4 mice and 5 muscles per group. (**B**) Exon skipping efficiency via systemic injection of PMO in *mdx* and *146aX* mice is not significantly different. Student's t-test. (**C**) Capillary-based immunoassay (Wes) was used to quantify dystrophin protein levels in skeletal muscle of *mdx* and *146aX* mice systemically treated with exon-skipping PMO via retroorbital injection. Depicted is a virtual Wes blot . (**C'**) Wes quantification of dystrophin protein levels in skeletal muscle. Dystrophin protein is significantly increased in *146aX* mice. Student's t-test, *p<0.05. Note: % Dystrophin was calculated by normalizing to the average *mdx* intensity for each muscle and setting it to 100%. (**D**) Dystrophin protein levels from Wes normalized to % *Dmd* exon skipped transcripts. There is a higher ratio of dystrophin restoration in *146aX* mice compared to *mdx* mice. Student's t-test, *p<0.05. (**E**) Dystrophin immunofluorescence (red) in PMO-injected *mdx* and *146aX* diaphragm and triceps muscles. Bar= 200mM and 100 mM, respectively. Muscles were counterstained with DAPI (nuclei) and laminin (green, not shown) to count total muscle fibers). (**E'**) Quantification of dystrophin-positive myofibers, (n=4 mice and 5 muscles per group). All muscles fibers were counter-stained with laminin (green, example shown in Figure S2C). The percentage of dystrophin-positive myofibers following PMO injection is significantly increased in *146aX* mice compared to mdx mice. Images were blinded during quantification. Student's t-test, *p<0.05. All data represented as mean ± S.E.M. Dia, diaphragm; TA, tibialis anterior; Quad, quadriceps; Gastroc, gastrocnemius; Tri, triceps.

Conflict of Interest

AAF has an issued patent on intellectual property relating to the manuscript (United States Patent #10266824).

Author Contributions

NM contributed to experiments, data analysis, manuscript writing and interpretation; KC performed data analysis; CT performed experiments and analysis, CH contributed to experimental design, writing and interpretation, AF contributed to experimental design, experiments, analysis, and manuscript writing.

Funding

CRH receives support from the Foundation to Eradicate Duchenne and the NIH (R01HL153054, R00HL130035, K99HL130035, L40AR068727). AAF receives support from the Foundation to Eradicate Duchenne, the Department of Defense (W81XWH-17-1-0475), and the NIH (L40AR070539 and L40NS127380).

Acknowledgements

We would like to thank Dr. Shin'ichi Takeda for the generous gift of the *mdx52* mice.

References

1. Hoffman EP, Brown RH, Jr., Kunkel LM. Dystrophin: the protein product of the Duchenne muscular dystrophy locus. Cell. 1987;51(6):919-28.
2. Beggs AH, Hoffman EP, Snyder JR, Arahata K, Specht L, Shapiro F, et al. Exploring the molecular basis for variability among patients with Becker muscular dystrophy: dystrophin gene and protein studies. Am J Hum Genet. 1991;49(1):54-67.
3. Hoffman EP, Kunkel LM, Angelini C, Clarke A, Johnson M, Harris JB. Improved diagnosis of Becker muscular dystrophy by dystrophin testing. Neurology. 1989;39(8):1011-7.
4. Kesari A, Pirra LN, Bremadesam L, McIntyre O, Gordon E, Dubrovsky AL, et al. Integrated DNA, cDNA, and protein studies in Becker muscular dystrophy show high exception to the reading frame rule. Hum Mutat. 2008;29(5):728-37.
5. van den Bergen JC, Wokke BH, Janson AA, van Duinen SG, Hulsker MA, Ginjaar HB, et al. Dystrophin levels and clinical severity in Becker muscular dystrophy patients. J Neurol Neurosurg Psychiatry. 2014;85(7):747-53.
6. Barp A, Bello L, Caumo L, Campadello P, Semplicini C, Lazzarotto A, et al. Muscle MRI and functional outcome measures in Becker muscular dystrophy. Sci Rep. 2017;7(1):16060.
7. Fiorillo AA, Heier CR, Novak JS, Tully CB, Brown KJ, Uaesoontrachoon K, et al. TNF-alpha-Induced microRNAs Control Dystrophin Expression in Becker Muscular Dystrophy. Cell Rep. 2015;12(10):1678-90.
8. Heier CR, McCormack NM, Tully CB, Novak JS, Newell-Stamper BL, Russell AJ, et al. The X-linked Becker muscular dystrophy (bmx) mouse models Becker muscular dystrophy via deletion of murine dystrophin exons 45-47. J Cachexia Sarcopenia Muscle. 2023.
9. Cirak S, Arechavala-Gomeza V, Guglieri M, Feng L, Torelli S, Anthony K, et al. Exon skipping and dystrophin restoration in patients with Duchenne muscular dystrophy after systemic phosphorodiamidate morpholino oligomer treatment: an open-label, phase 2, dose-escalation study. Lancet. 2011;378(9791):595-605.
10. Frank DE, Schnell FJ, Akana C, El-Husayni SH, Desjardins CA, Morgan J, et al. Increased dystrophin production with golodirsen in patients with Duchenne muscular dystrophy. Neurology. 2020;94(21):e2270-e82.
11. Wagner KR, Kuntz NL, Koenig E, East L, Upadhyay S, Han B, et al. Safety, tolerability, and pharmacokinetics of casimersen in patients with Duchenne muscular dystrophy amenable to exon 45 skipping: A randomized, double-blind, placebo-controlled, dose-titration trial. Muscle Nerve. 2021;64(3):285-92.
12. Clemens PR, Rao VK, Connolly AM, Harper AD, Mah JK, McDonald CM, et al. Efficacy and Safety of Viltolarsen in Boys With Duchenne Muscular Dystrophy: Results From the Phase 2, Open-Label, 4-Year Extension Study. J Neuromuscul Dis. 2023.
13. Study of Eteplirsen in DMD Patients (PROMOVI).
14. Servais L, Mercuri E, Straub V, Guglieri M, Seferian AM, Scoto M, et al. Long-Term Safety and Efficacy Data of Golodirsen in Ambulatory Patients with Duchenne Muscular Dystrophy Amenable to Exon 53 Skipping: A First-in-human, Multicenter, Two-Part, Open-Label, Phase 1/2 Trial. Nucleic Acid Ther. 2022;32(1):29-39.
15. Eisenberg I, Eran A, Nishino I, Moggio M, Lamperti C, Amato AA, et al. Distinctive patterns of microRNA expression in primary muscular disorders. Proc Natl Acad Sci U S A. 2007;104(43):17016-21.
16. Cacchiarelli D, Incitti T, Martone J, Cesana M, Cazzella V, Santini T, et al. miR-31 modulates dystrophin expression: new implications for Duchenne muscular dystrophy therapy. EMBO Rep. 2011;12(2):136-41.
17. Humphreys DT, Westman BJ, Martin DI, Preiss T. MicroRNAs control translation initiation by inhibiting eukaryotic initiation factor 4E/cap and poly(A) tail function. Proc Natl Acad Sci U S A. 2005;102(47):16961-6.

18. Taganov KD, Boldin MP, Chang KJ, Baltimore D. NF-kappaB-dependent induction of microRNA miR-146, an inhibitor targeted to signaling proteins of innate immune responses. Proc Natl Acad Sci U S A. 2006;103(33):12481-6.
19. Heier CR, Fiorillo AA, Chaisson E, Gordish-Dressman H, Hathout Y, Damsker JM, et al. Identification of Pathway-Specific Serum Biomarkers of Response to Glucocorticoid and Infliximab Treatment in Children with Inflammatory Bowel Disease. Clin Transl Gastroenterol. 2016;7(9):e192.
20. Fiorillo AA, Tully CB, Damsker JM, Nagaraju K, Hoffman EP, Heier CR. Muscle miRNAome shows suppression of chronic inflammatory miRNAs with both prednisone and vamorolone. Physiol Genomics. 2018;50(9):735-45.
21. Araki E, Nakamura K, Nakao K, Kameya S, Kobayashi O, Nonaka I, et al. Targeted disruption of exon 52 in the mouse dystrophin gene induced muscle degeneration similar to that observed in Duchenne muscular dystrophy. Biochem Biophys Res Commun. 1997;238(2):492-7.
22. Lu LF, Boldin MP, Chaudhry A, Lin LL, Taganov KD, Hanada T, et al. Function of miR-146a in controlling Treg cell-mediated regulation of Th1 responses. Cell. 2010;142(6):914-29.
23. Mann CJ, Honeyman K, Cheng AJ, Ly T, Lloyd F, Fletcher S, et al. Antisense-induced exon skipping and synthesis of dystrophin in the mdx mouse. Proc Natl Acad Sci U S A. 2001;98(1):42-7.
24. Aoki Y, Nakamura A, Yokota T, Saito T, Okazawa H, Nagata T, et al. In-frame dystrophin following exon 51-skipping improves muscle pathology and function in the exon 52-deficient mdx mouse. Mol Ther. 2010;18(11):1995-2005.
25. Soutschek M, Gross F, Schratt G, Germain PL. scanMiR: a biochemically based toolkit for versatile and efficient microRNA target prediction. Bioinformatics. 2022;38(9):2466-73.
26. Grimson A, Farh KK, Johnston WK, Garrett-Engele P, Lim LP, Bartel DP. MicroRNA targeting specificity in mammals: determinants beyond seed pairing. Mol Cell. 2007;27(1):91-105.
27. Novak JS, Spathis R, Dang UJ, Fiorillo AA, Hindupur R, Tully CB, et al. Interrogation of Dystrophin and Dystroglycan Complex Protein Turnover After Exon Skipping Therapy. J Neuromuscul Dis. 2021;8(s2):S383-S402.
28. Li D, Yue Y, Duan D. Preservation of muscle force in Mdx3cv mice correlates with low-level expression of a near full-length dystrophin protein. Am J Pathol. 2008;172(5):1332-41.
29. Li D, Yue Y, Duan D. Marginal level dystrophin expression improves clinical outcome in a strain of dystrophin/utrophin double knockout mice. PLoS One. 2010;5(12):e15286.
30. van Putten M, Hulsker M, Nadarajah VD, van Heiningen SH, van Huizen E, van Iterson M, et al. The effects of low levels of dystrophin on mouse muscle function and pathology. PLoS One. 2012;7(2):e31937.
31. Phelps SF, Hauser MA, Cole NM, Rafael JA, Hinkle RT, Faulkner JA, et al. Expression of full-length and truncated dystrophin mini-genes in transgenic mdx mice. Hum Mol Genet. 1995;4(8):1251-8.
32. Godfrey C, Muses S, McClorey G, Wells KE, Coursindel T, Terry RL, et al. How much dystrophin is enough: the physiological consequences of different levels of dystrophin in the mdx mouse. Hum Mol Genet. 2015;24(15):4225-37.
33. Clemens PR, Rao VK, Connolly AM, Harper AD, Mah JK, Smith EC, et al. Safety, Tolerability, and Efficacy of Viltolarsen in Boys With Duchenne Muscular Dystrophy Amenable to Exon 53 Skipping: A Phase 2 Randomized Clinical Trial. JAMA Neurol. 2020;77(8):982-91.
34. Hildyard JC, Wells DJ. Investigating Synthetic Oligonucleotide Targeting of Mir31 in Duchenne Muscular Dystrophy. PLoS Curr. 2016;8.
35. Vila MC, Klimek MB, Novak JS, Rayavarapu S, Uaesoontrachoon K, Boehler JF, et al. Elusive sources of variability of dystrophin rescue by exon skipping. Skelet Muscle. 2015;5:44.

36. Kinder TB, Heier CR, Tully CB, Van der Muelen JH, Hoffman EP, Nagaraju K, et al. Muscle Weakness in Myositis: MicroRNA-Mediated Dystrophin Reduction in a Myositis Mouse Model and Human Muscle Biopsies. Arthritis Rheumatol. 2020;72(7):1170-83.
37. Nunes AM, Ramirez M, Jones TI, Jones PL. Identification of candidate miRNA biomarkers for facioscapulohumeral muscular dystrophy using DUX4-based mouse models. Dis Model Mech. 2021;14(8).
38. Moran-Moguel MC, Petarra-Del Rio S, Mayorquin-Galvan EE, Zavala-Cerna MG. Rheumatoid Arthritis and miRNAs: A Critical Review through a Functional View. J Immunol Res. 2018;2018:2474529.
39. Reale M, D'Angelo C, Costantini E, Laus M, Moretti A, Croce A. MicroRNA in Sjogren's Syndrome: Their Potential Roles in Pathogenesis and Diagnosis. J Immunol Res. 2018;2018:7510174.
40. Chapman CG, Pekow J. The emerging role of miRNAs in inflammatory bowel disease: a review. Therap Adv Gastroenterol. 2015;8(1):4-22.
41. Batra SK, Heier CR, Diaz-Calderon L, Tully CB, Fiorillo AA, van den Anker J, et al. Serum miRNAs Are Pharmacodynamic Biomarkers Associated With Therapeutic Response in Pediatric Inflammatory Bowel Disease. Inflamm Bowel Dis. 2020;26(10):1597-606.
42. Elnady HG, Sherif LS, Kholoussi NM, Ali Azzam M, Foda AR, Helwa I, et al. Aberrant Expression of Immune-related MicroRNAs in Pediatric Patients with Asthma. Int J Mol Cell Med. 2020;9(4):246-55.
43. Boldin MP, Taganov KD, Rao DS, Yang L, Zhao JL, Kalwani M, et al. miR-146a is a significant brake on autoimmunity, myeloproliferation, and cancer in mice. J Exp Med. 2011;208(6):1189-201.
44. Nahid MA, Pauley KM, Satoh M, Chan EK. miR-146a is critical for endotoxin-induced tolerance: IMPLICATION IN INNATE IMMUNITY. J Biol Chem. 2009;284(50):34590-9.
45. Wang S, Yang Y, Suen A, Zhu J, Williams B, Hu J, et al. Role of extracellular microRNA-146a-5p in host innate immunity and bacterial sepsis. iScience. 2021;24(12):103441.
46. Bronisz-Budzynska I, Chwalenia K, Mucha O, Podkalicka P, Karolina Bukowska S, Jozkowicz A, et al. miR-146a deficiency does not aggravate muscular dystrophy in mdx mice. Skelet Muscle. 2019;9(1):22.
47. Diener C, Keller A, Meese E. Emerging concepts of miRNA therapeutics: from cells to clinic. Trends Genet. 2022;38(6):613-26.
48. Taubel J, Hauke W, Rump S, Viereck J, Batkai S, Poetzsch J, et al. Novel antisense therapy targeting microRNA-132 in patients with heart failure: results of a first-in-human Phase 1b randomized, double-blind, placebo-controlled study. Eur Heart J. 2021;42(2):178-88.
49. van der Ree MH, van der Meer AJ, van Nuenen AC, de Bruijne J, Ottosen S, Janssen HL, et al. Miravirsen dosing in chronic hepatitis C patients results in decreased microRNA-122 levels without affecting other microRNAs in plasma. Aliment Pharmacol Ther. 2016;43(1):102-13.
50. Abplanalp WT, Fischer A, John D, Zeiher AM, Gosgnach W, Darville H, et al. Efficiency and Target Derepression of Anti-miR-92a: Results of a First in Human Study. Nucleic Acid Ther. 2020;30(6):335-45.
51. Cerro-Herreros E, Gonzalez-Martinez I, Moreno-Cervera N, Overby S, Perez-Alonso M, Llamusi B, et al. Therapeutic Potential of AntagomiR-23b for Treating Myotonic Dystrophy. Mol Ther Nucleic Acids. 2020;21:837-49.
52. Overby SJ, Cerro-Herreros E, Gonzalez-Martinez I, Varela MA, Seoane-Miraz D, Jad Y, et al. Proof of concept of peptide-linked blockmiR-induced MBNL functional rescue in myotonic dystrophy type 1 mouse model. Mol Ther Nucleic Acids. 2022;27:1146-55.